



## Time-Based Network Analysis Before and After the $M_w$ 8.3 Illapel Earthquake 2015 Chile

DENISSE PASTÉN,<sup>1,2</sup> FELIPE TORRES,<sup>1,3</sup> BENJAMÍN TOLEDO,<sup>1</sup> VÍCTOR MUÑOZ,<sup>1</sup> JOSÉ ROGAN,<sup>1,3</sup> and  
JUAN ALEJANDRO VALDIVIA<sup>1,3</sup>

**Abstract**—A complex network analysis of the seismic activity in the central zone of Chile is made, where each node corresponds to a location, where a seism occurs. The  $M_w = 8.3$  Illapel earthquake (16 September 2015) is included in the data set studied. Assuming a self-similar data network, the value of the power law characteristic exponent  $\gamma$  for the link probability distribution of the directed network and the value of the power law characteristic exponent  $\delta$  for the cumulative distribution of the betweenness centrality are studied, before and after the earthquake. Both exponents have a different values before and after the earthquake when the network is built with cell size of  $5 \times 5 \times 5$  km, but there is no difference when the cell size is  $10 \times 10 \times 10$  km. The exponents were evaluated for the data set with the total number of seismic events and for three cutoffs in magnitude. There is not much variation when applying the cutoff. Variations of both exponents are found when both subsets, before and after the main event, are compared, suggesting that the topological features of the complex network of seisms are modified by major events.

**Key words:** Complex networks, Illapel, Earthquake.

### 1. Introduction

The study of complex networks has an important development in the last years, and it is becoming a useful tool that has been applied to many systems real systems, providing new perspectives in diverse fields, such as communication, biology, and social relationships (ALBERT *et al.* 1999; ALON 2003; BARABÁSI *et al.* 2000; BARABÁSI and OLTVAI 2004; BAR-JOSEPH *et al.* 2003; CENTOLA 2010; PALLA *et al.* 2005). These

types of analyses have been particularly fruitful in the study of earthquakes (COSTA *et al.* 2005; DOROGOVTSSEV and MENDES 2003; DOROGOVTSSEV *et al.* 2008; GERMANO and MOURA 2006; GHAFFARI and YOUNG 2013; GRUZD *et al.* 2011; KITSACK *et al.* 2007; LACASA *et al.* 2009; NEWMAN 2002, 2005; NEWMAN and GIRVAN 2004; ABE and SUZUKI 2006; TELESKA and LOVALLO 2012), an interesting and difficult system to understand. Seismic data can be studied as a complex network considering its spatial distribution (ABE and SUZUKI 2006; ABE *et al.* 2011) or, more recently, as a visibility graph (AGUILAR-SANJUAN and VARGAS 2013; TELESKA and LOVALLO 2012). In the former approach, the spatial network of seismic data has usually found to be scale-free and small world (ABE and SUZUKI 2006, 2004; ABE *et al.* 2011, 2010). In the later approach, the magnitude is included in the analysis, and it also seems to display scale-free behavior (AGUILAR-SANJUAN and VARGAS 2013; TELESKA and LOVALLO 2012). In this study, we have analyzed a seismic data set measured in the central zone of Chile considering it as a spatial complex network. In our approach, we have divided the data in two different sets according to the time of the main event, before and after the large earthquake of Illapel 2015, and the exponents for the probability distribution of connectivity and the cumulative distribution of betweenness were calculated and compared before and after the  $M_w = 8.3$  earthquake, for the total number of seismic events and three magnitude thresholds. It is important to mention that following BARTHELEMY (2004), it is necessary to analyze both the probability distribution of connectivity and the cumulative distribution of betweenness to assert the scale-free properties of a complex network.

<sup>1</sup> Departamento de Física, Facultad de Ciencias, Universidad de Chile, Santiago, Chile. E-mail: denisse.pasten.g@gmail.com

<sup>2</sup> AG2E, Advanced Mining Technology Center, Facultad de Ciencias Físicas y Matemáticas, Universidad de Chile, Santiago, Chile.

<sup>3</sup> Centro para la Nanociencia y la Nanotecnología, Los Andes, Chile.

## 2. Data and Network Analysis

The data set was obtained from the National Seismological Center of Chile (Centro Sismológico Nacional, CSN) between October 2000 and October 2015, containing 15 years of measurements with 34,877 seismic events in the zone between  $29^\circ$  and  $35.5^\circ$  South Latitude and between  $69^\circ$  and  $74^\circ$  West Longitude, as shown in Fig. 1. This includes the Illapel earthquake, occurred on 16 September 2015, with magnitude  $M_w = 8.3$ , as reported by the CSN.

To use the hypocenter in kilometers, the latitude,  $\theta$ , and the longitude,  $\phi$ , were converted to kilometers following the expressions:

$$\begin{aligned} d_i^{NS} &= R(\theta_i - \theta_0), \\ d_i^{EW} &= R(\phi_i - \phi_0) \cos(\theta_{\text{prom}}), \\ d_i^z &= z_i, \end{aligned} \quad (1)$$

where  $z_i$  is the depth in km,  $\theta_0$  is the minimum latitude,  $\theta_{\text{prom}}$  is the average latitude for the data set studied,  $\phi_0$  is the minimum longitude, and  $R$  is the radius of the Earth, considered for this study as 6370 km (ABE and SUZUKI 2006; ABE *et al.* 2011).



Figure 1

Map of the zone studied, for seismic events with  $M_w \geq 4$

A complete set in magnitude is obtained for this data starting from  $M_w = 3.0$ , beyond which the Gutenberg–Richter law is satisfied, as can be seen in Fig. 2.

Furthermore, the original data set was divided in two sets, before and after the large Illapel earthquake. The data set before the 8.3 earthquake considers until 15 September 2015, and contains 33,209 events, while the data set after the earthquake starts on 16 September 2015, and contains 1668 seismic events. We will be interested in studying the dependence of our analysis with the magnitude threshold, and hence, three magnitude thresholds were used:  $M_w = 3.0$  (the complete set in magnitude);  $M_w = 3.5$ ; and  $M_w = 4.0$ . In this way, we intend to study variations of our results when the size of the data set is reduced, and statistics become poorer.

Using these data, a complex network is constructed following the procedure described in ABE and SUZUKI (2006) and ABE *et al.* (2011), and which we summarize below. A cubic grid of cells of equal-size  $\Delta$ , covering the geographical zone of interest, is considered. If a cell contains a seismic event, it is considered as a node of our network, and the links between nodes map the time sequence of the data. Hence, the first seismic event yields the first node of the network, then a link is directed from the first node to the second one (the cell where the second seismic event occurred), and so on.

Thus, we can study the dependence of the topological features of the networks with time (before/

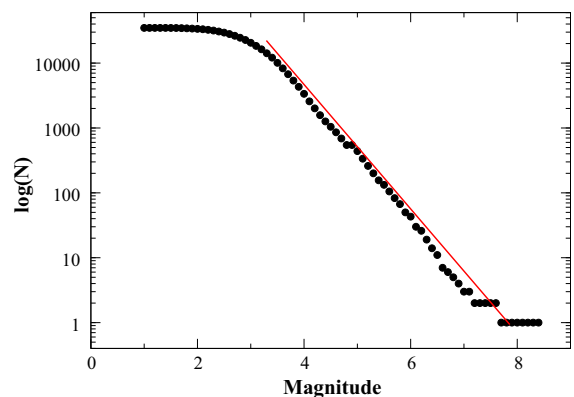


Figure 2

Complete magnitude data set is found above  $M_w = 3.0$ , with the parameter  $b = 0.90 \pm 0.01$

after a major seismic event), and with grid size  $\Delta$ . In this work, we will analyze the scale-free properties of these 2 networks (ABE and SUZUKI 2004, 2006; BAIESI and PACZUSKI 2004) by studying their probability distribution of connectivity and the cumulative distribution of betweenness centrality, as both distributions need to follow power laws to be scale-free networks (BARTHELEMY 2004).

The connectivity is defined as the number of links that each node has. In a scale-free network, the probability distribution for the connectivity,  $P(k)$ , follows a power law:

$$P(k) = k^{-\gamma}, \quad (2)$$

where  $\gamma$  is the characteristics exponent and, for real seismic networks, usually has a value close to 2 (TELESCA and LOVALLO 2012; AGUILAR-SANJUAN and VARGAS 2013).

Similarly, the betweenness centrality (BC) is a measure of how important is the node  $m$  in the shortest distance connections between all the other

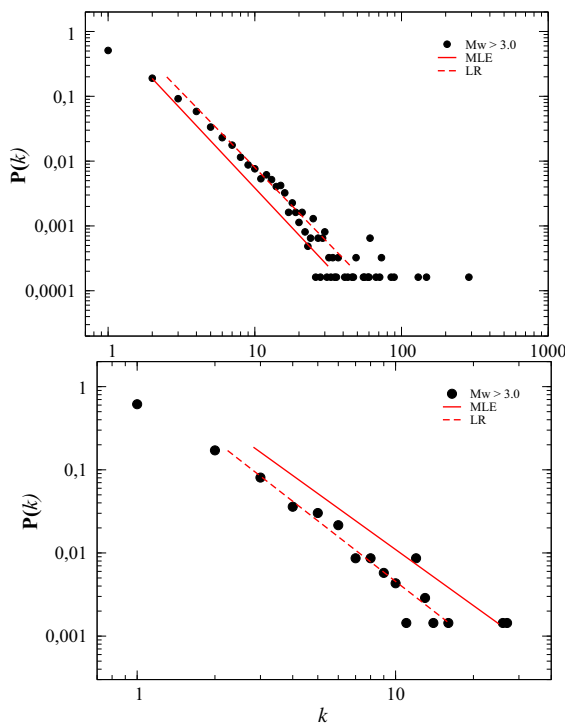


Figure 3

Probability distribution of connectivity before the large earthquake (*upper panel*) and after the large earthquake (*lower panel*), for the data points with magnitude greater than 3.0. Cell size is 10 km

pairs of nodes. Hence, if the BC is large, the nodes are more active. The cumulative distribution of BC turns out to follow a power law if

$$B(x < g) \sim g^{-\delta}. \quad (3)$$

In all cases, our analysis consists of calculating the characteristic exponent,  $\gamma$ , of the scale-free connectivity distribution of the network, and  $\delta$  for the cumulative distribution of the betweenness centrality.

### 2.1. Maximum Likelihood Estimation and Linear Regression

Hence, in this study, it is necessary to calculate the slope of power law distributions: the probability distribution of the connectivity and the cumulative probability distribution of the betweenness centrality. To obtain a reliable estimation for a power law distribution is not a simple task, specially for a

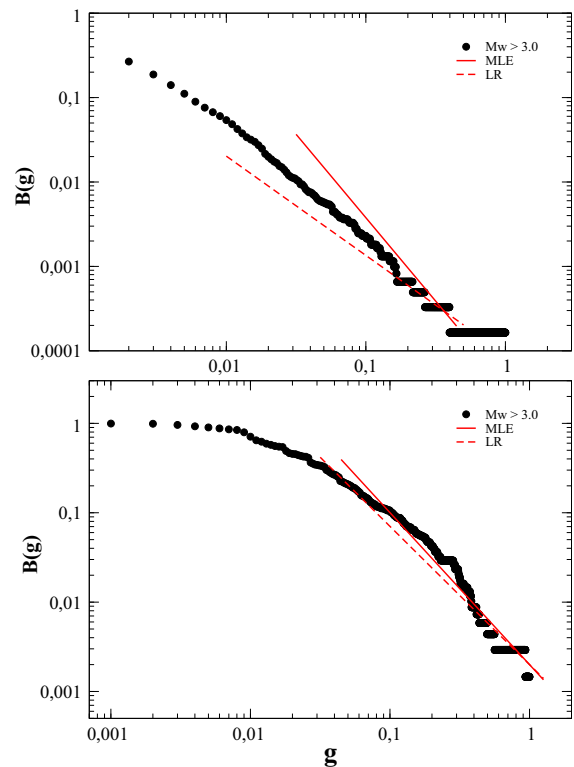


Figure 4

Probability distribution of betweenness centrality before the large earthquake (*upper panel*) and after the large earthquake (*lower panel*), for the data points with magnitude greater than 3.0. Cell size is 10 km

Table 1

Table with the values of  $\gamma$  and  $\delta$  for the magnitude threshold  $M_w > 3.0$ , and a cell size,  $\Delta = 10$  km, before and after the Illapel 2015 earthquake

Values of the critical exponents, $\gamma$ and $\delta$ for two methods of fitting							
$\Delta$ (km)	$M_w$	Parameter	LR	MLE	Minimum	$N$	$N_{\text{fit}}$
10	3.0	$\gamma$ before	$2.3 \pm 0.2$	$2.4 \pm 0.1$	6	56	46
		$\gamma$ after	$2.4 \pm 0.3$	$2.2 \pm 0.2$	2	18	10
10	3.0	$\delta$ before	$1.18 \pm 0.03$	$1.98 \pm 0.05$	0.002	999	23
		$\delta$ after	$1.55 \pm 0.01$	$1.7 \pm 0.2$	0.06	999	338

LR indicates the values calculated using linear regression, and MLE using the maximum likelihood estimation. This table shows the minimum value of  $k$  and BC used (to calculate  $\gamma$  and  $\delta$ , respectively); the number of points in the subset above the magnitude threshold,  $N$ ; and the number of points used for the fit, as demanded by the Kolmogorov–Smirnov test,  $N_{\text{fit}}$

Table 2

Table with the values of  $\gamma$  for the different magnitude thresholds, and two values of the cell size,  $\Delta = 5$  km and  $\Delta = 10$  km, before the Illapel 2015 earthquake

Values of $\gamma$ exponent before $M_w = 8.3$ Illapel earthquake					
$\Delta$ (km)	$M_w$	$\gamma$	Minimum	$N$	$N_{\text{fit}}$
5	3.0	$3.0 \pm 0.1$	2	34	18
	3.5	$3.2 \pm 0.1$	2	20	12
	4.0	$4.0 \pm 0.1$	2	7	5
10	3.0	$2.2 \pm 0.1$	2	56	46
	3.5	$2.3 \pm 0.1$	2	35	28
	4.0	$2.5 \pm 0.1$	2	14	6

Columns have the same meaning as in Table 1

Table 3

Table with the values of  $\gamma$  for the different magnitude thresholds, and two values of the cell size,  $\Delta = 5$  km and  $\Delta = 10$  km, after the Illapel 2015 earthquake

Values of $\gamma$ exponent after $M_w = 8.3$ Illapel earthquake					
$\Delta$ (km)	$M_w$	$\gamma$	Minimum	$N$	$N_{\text{fit}}$
5	3.0	$3.6 \pm 0.2$	2	9	6
	3.5	$3.8 \pm 0.3$	2	9	9
	4.0	$4.2 \pm 0.4$	2	7	4
10	3.0	$2.2 \pm 0.1$	2	18	10
	3.5	$2.1 \pm 0.1$	2	13	11
	4.0	$2.6 \pm 0.3$	2	9	6

Columns have the same meaning as in Table 1

relatively small number of points. To decide the most reliable method to fit, these two distributions for these two particular data sets (before and after the Illapel earthquake, respectively), we now apply two commonly used strategies to produce an estimation of the

power law index, namely, the maximum likelihood estimation (MLE) and the linear regression (LR).

To compute the MLE estimation, we use the approach proposed by GOLDSTEIN *et al.* (2004) for discrete (connectivity) or continuous (betweenness

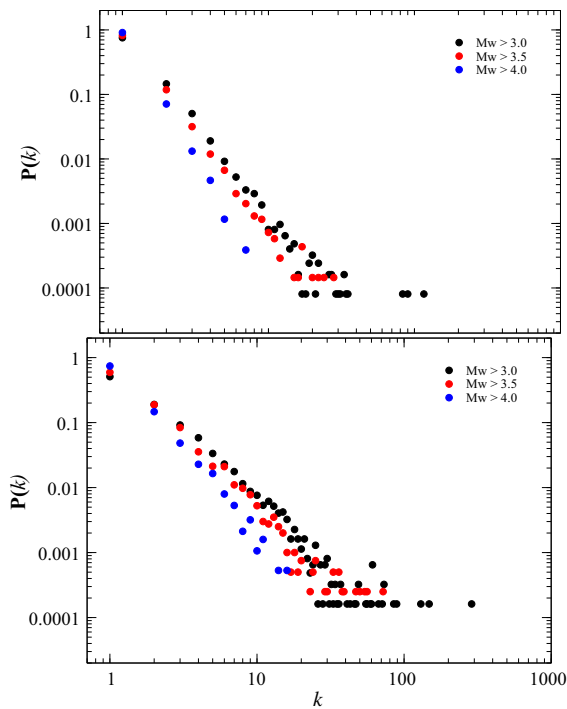


Figure 5

Probability distribution of connectivity for two cell sizes, 5 km (*upper panel*) and 10 km (*lower panel*), before the Illapel earthquake. Three magnitude thresholds are considered, as indicated in the figure

centrality) data produced with a scale-free distribution, where the range of applicability of the estimated scale-free distribution is found from the Kolmogorov–Smirnov type of test proposed by GOLDSTEIN *et al.* (2004). For the LR, we apply a simple linear regression analysis in log–log scale of the histogram obtained from the connectivity of betweenness centrality distribution of the complex network constructed for each of the two data sets. We use the same range of values demanded by the Kolmogorov–Smirnov test of the MLE.

In Figs. 3 and 4, we show a comparison of the connectivity distribution and the estimations produced with the MLE and LR methods, corresponding to the complex networks constructed from the two data sets (before and after the earthquake) with  $\Delta = 10$  km and  $M_w \geq 3.0$ . The values of the slopes and points used are shown in Table 1. For the connectivity, the applicability range was  $10^{0.8} \leq k \leq 10^{1.8}$  before the large seismic event, while for the data after the large earthquake, we found  $10^{0.4} \leq k \leq 10^{1.2}$ . For the

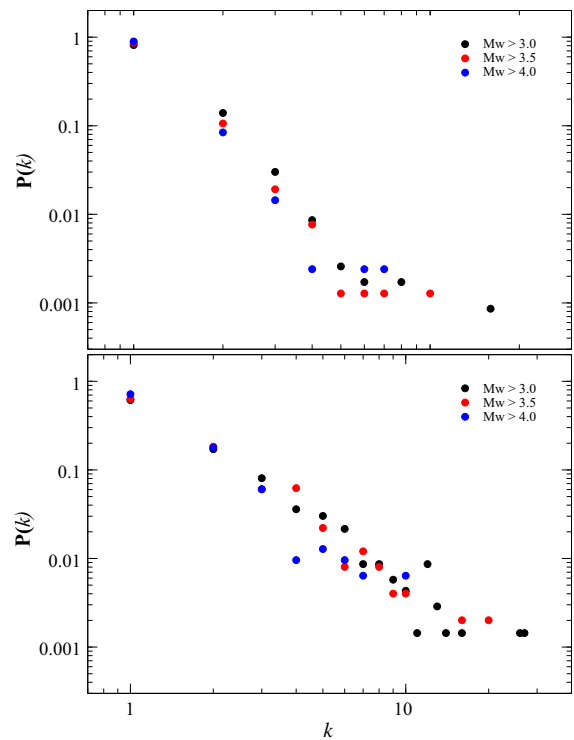


Figure 6

Probability distribution of connectivity for two cell sizes, 5 km (*upper panel*) and 10 km (*lower panel*), after the Illapel earthquake. Three magnitude thresholds are considered, as indicated in the figure

betweenness centrality, the same Kolmogorov–Smirnov test was used, with the ranges  $10^{-3.0} \leq g \leq 10^{-1.0}$  before the large earthquake, and  $10^{-1.2} \leq g \leq 10^{-0.4}$  after the large seismic event.

The values of  $\gamma$  are quite similar for both methods, but the values of  $\delta$  are very different. On the other hand, the number of data points included in the range of applicability demanded by the Kolmogorov–Smirnov method may be quite small, as shown in Table 1. Similarly, the error obtained for BC is smaller using LR than the error using MLE.

We note that when the data have a reasonably large number of points (e.g., data set before the earthquake), both methods seem to provide similar estimations for the power law index; however, when we have a relatively small number of data points (e.g., data set after the earthquake), the estimations of the power law index are not as similar. One of the main problems is that the Kolmogorov–Smirnov type of test for the MLE sometimes demands a very small

Table 4

Table with the values of  $\delta$ , the characteristic exponent for the cumulative distribution of BC, for the set with the total number of seismic events and the three subsets with different magnitude thresholds and two values of the cell size,  $\Delta = 5$  km and  $\Delta = 10$  km, before the Illapel 2015 earthquake

Values of $\delta$ exponent before $M_w = 8.3$ Illapel earthquake					
$\Delta$ (km)	$M_w$	$\delta$	Minimum	$N$	$N_{\text{fit}}$
5	3.0	$1.43 \pm 0.01$	0.006	999	193
	3.5	$1.48 \pm 0.01$	0.006	999	114
	4.0	$2.02 \pm 0.02$	0.05	999	150
10	3.0	$1.45 \pm 0.01$	0.02	999	680
	3.5	$1.42 \pm 0.01$	0.02	999	280
	4.0	$1.26 \pm 0.01$	0.02	999	280

Columns have the same meaning as in Table 1

Table 5

Table with the values of  $\delta$ , the characteristic exponent of the cumulative distribution for BC. This exponent was calculated for the set with the total number of seismic events and the three subsets with different magnitude thresholds and two values of the cell size,  $\Delta = 5$  km and  $\Delta = 10$  km, after the Illapel 2015 earthquake

Values of $\delta$ exponent after $M_w = 8.3$ Illapel earthquake					
$\Delta$ (km)	$M_w$	$\delta$	Minimum	$N$	$N_{\text{fit}}$
5	3.0	$2.29 \pm 0.02$	0.02	999	480
	3.5	$2.02 \pm 0.01$	0.03	994	770
	4.0	$1.82 \pm 0.01$	0.03	999	370
10	3.0	$2.31 \pm 0.02$	0.25	999	550
	3.5	$2.32 \pm 0.04$	0.25	999	550
	4.0	$1.75 \pm 0.01$	0.05	997	750

Columns have the same meaning as in Table 1

range of applicability of the power law distribution, which, in essence, can restrict considerably the number of points over which the MLE estimation is done. Hence, for the complex networks produced by our data sets, the LR seems to give a more reliable result than the MLE, and gives us the possibility to use a larger range of values to make the fitting. Therefore, for the rest of the manuscript, we will use the LR to estimate  $\gamma$  for the connectivity and  $\delta$  for the BC, respectively. The applicability range of values used to calculate the slope was defined by minimizing the fitting error  $\sigma$  for the LR.

### 3. Variability of the Complex Networks

We will now analyze the variation of the scale-free properties of the complex networks computed after and before the large earthquake of Illapel, as we

change  $\Delta$  and the magnitude thresholds  $M_w$ , using the LR method to estimate the power law index as suggested above. We show, in Tables 2 and 3, the estimated value of  $\gamma$ , before and after the large earthquake, respectively, for threshold values of  $M_w \geq 3.0$ , 3.5, and 4.0; for  $\Delta = 5$  km and  $\Delta = 10$  km.

Focusing on data for thresholds  $M_w > 3.0$  and 3.5 in Tables 2 and 3, we notice that, in general, similar values of  $\gamma$  are obtained. On the other hand, a large variation of  $\gamma$  is found when data before and after the Illapel earthquake are compared, at least for  $\Delta = 5$  km. This suggests that the topological features of the network are affected by the occurrence of a large earthquake, specially at these small scales.

The values of the slope for the sets with  $M_w > 4.0$  do not have such a regular behavior. Comparing data sets before and after the earthquake, for both cell sizes, the values of  $\gamma$  are almost the same.

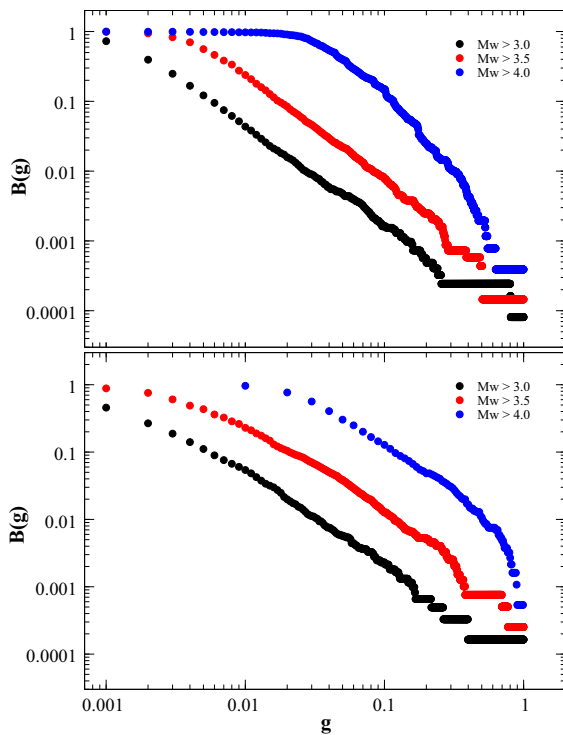


Figure 7

Cumulative distribution of BC for the seismic network before the large  $M_w$  8.3 earthquake, considering two cell sizes, 5 km (*upper panel*) and 10 km (*lower panel*). Three magnitude thresholds were considered

The connectivity distributions, with the estimated LR distributions, are shown in Figs. 5 and 6. We clearly note that the connectivity distribution, even for different magnitude thresholds, has a power law tail. However, to assert the scale-free nature of the complex networks, it is important to analyze the power law characteristics of the BC distributions, to which we now turn.

Before the earthquake,  $\delta$  is close to 1.4 for both cell sizes. After the earthquake,  $\delta$  is close to 2.0 for  $\Delta = 5$  km, and close to 2.3 for  $\Delta = 10$  km. The values of  $\delta$  for both cell sizes, using the linear regression method and all thresholds, are shown in Tables 4 (before the earthquake), and 5 (after the earthquake).

Consistent with the findings in the previous section, the case  $M_w > 4.0$  does not show the same regular behavior. It can be seen in Tables 4 and 5 that the slopes are not similar. This holds for both cell

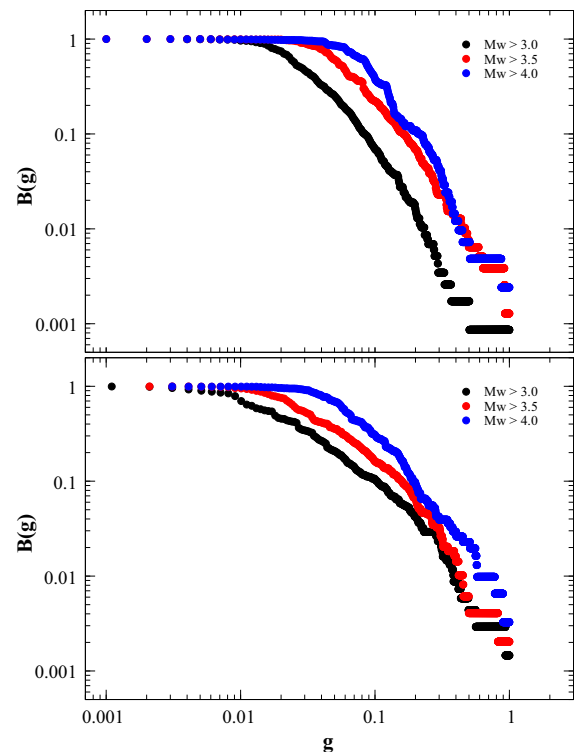


Figure 8

Cumulative distribution BC for two cell sizes after the large  $M_w$  8.3 Illapel earthquake, 5 km (*upper panel*) and 10 km (*lower panel*). The BC were calculated for three magnitude thresholds

sizes, but specially for the smaller one, namely  $\Delta = 5$  km.

Focusing now on thresholds  $M_w > 3.0$  and  $M_w > 3.5$ , important differences exist between the slopes of the cumulative distribution of BC before and after the  $M_w$  8.3 earthquake. This jump in the values of  $\delta$  when the sets before and after the large seismic event are compared suggests that the  $M_w$  8.3 Illapel earthquake modifies the shortest paths between nodes of the network.

#### 4. Discussion

We have characterized the seismicity in the central zone of Chile before and after the  $M_w$  8.3 Illapel earthquake using a complex network description, where each node corresponds to a cubic cell, where an hypocenter is located.

A jump in the value of the characteristic exponent of the connectivity distribution,  $\gamma$ , is found when data before and after the seism are compared. However, this behavior is found only for the smaller cell size  $\Delta = 5$  km, not  $\Delta = 10$  km. Thus, the large earthquake seems to change the network connectivity, making more connections between aftershocks, at least at this smaller scale.

In addition, the value of the characteristic exponent for the cumulative distribution of the betweenness centrality of the network shows an evident change before/after the earthquake for both cell sizes (Figs. 7, 8).

The above results are clear for networks built with seisms above  $M_w = 3.0$  and  $M_w = 3.5$  magnitude thresholds. When only  $M_w > 4.0$  seisms are considered, the behavior of  $\gamma$  and  $\delta$  is not so clear, which could be due to the small number of data points, and thus poorer statistics, in both data sets.

### 5. Concluding Remarks

Two directed networks were constructed for the data set measured in the central zone of Chile, including the  $M_w$  8.3 Illapel earthquake. This study considered an analysis of the characteristic exponents  $\gamma$  (probability distribution of connectivity) and  $\delta$  (cumulative distribution of betweenness centrality).

The most interesting result is the jump in the values of  $\gamma$  and  $\delta$  after the large earthquake, suggesting that the earthquake modifies the network, a remarkable fact, as this data set considers 15 years of measurements in an area quite greater than the area close to the large seismic event. In the end, the effect of the 8.3 Illapel earthquake reached almost 700 km to the south of the hypocenter and 400 km to the east of the hypocenter, generating a new network in the total area of study.

Finally, at least for the  $M_w \geq 3.0$  threshold, we can say that our results strongly suggest that complex networks constructed before and after the large Illapel earthquake are scale-free, as the values of  $\gamma$  and  $\delta$  satisfy the restrictions imposed by BARTHELEMY (2004).

### Acknowledgments

This work was supported by the Fondo Nacional de Investigaciones Científicas y Tecnológicas (FONDECYT) under grants No 1130272 and No 1120599 (JR), No 1150718 (JAV), No 1130273 (BT), No 1121144 and 1161711 (VM), and No 1150806 (FT). We thank the support of CEDENNA through “Financiamiento Basal para Centros Científicos y Tecnológicos de Excelencia” FB0807 (FT, JR, JAV). We also thank financial support of project Anillo Conicyt Pia ACT1405 (JR, VM, JAV). DP wants to thank Sandeep Kumar for his valuable help.

### REFERENCES

- S. ABE, N. SUZUKI, *Scale-free network of earthquakes*. Europhys. Lett. 65(4), 581–586 (2004)
- S. ABE, D. PASTÉN, N. SUZUKI, *Finite data-size scaling of clustering in earthquake networks*. Physica A 390, 7 (2010)
- S. ABE, D. PASTÉN, V. MUÑOZ, N. SUZUKI, *Universalities of earthquake-network characteristics*. Chinese Science Bulletin 56, 34 (2011)
- S. ABE, N. SUZUKI, *Complex-network description of seismicity*. Nonlinear Proc. Geophys. 13, 145–150 (2006)
- B. AGUILAR-SANJUAN, L.G. VARGAS, *Earthquake magnitude time series: scaling behavior of visibility networks*. Eur. Phys. J. B 86, 454 (2013)
- R. ALBERT, H. JEONG, L. BARABASI, *Diameter of the world wide web*. Nature 401, 130–131 (1999)
- U. ALON, *Biological networks: the tinkerer as engineer*. Science 301, 1866–1867 (2003)
- M. BAIESI, M. PACZUSKI, *Scale-free networks of earthquakes and aftershocks*. Phys. Rev. E 69, 066106 (2004)
- Z. BAR-JOSEPH, G.K. GERBER, T.I. LEE, N.J. RINALDI, J.Y. YOO, F. ROBERT, D.B. GORDON, E. FRAENKEL, T.S. JAACKLOA, R.A. YOUNG, D.K. GIFFORD., *Computational discovery of gene modules and regulatory networks*21, 1337–1342 (2003)
- A.-L. BARABÁSI, Z.N. OLTVAI, *Network biology: understanding the cell’s functional organization*. Nature Reviews Genetics 5, 101–113 (2004)
- A.-L. BARABÁSI, R. ALBERT, H. JEONG, *Scale-free characteristics of random networks: the topology of the world-wide web*. Phys. A 281, 69–77 (2000)
- M. BARTHELEMY, *Betweenness centrality in large complex networks*. Eur. Phys. J. B 38, 163–168 (2004)
- D. CENTOLA, *The spread behavior in an online social network experiment*. Science 329, 1194–1197 (2010)
- L. da F. COSTA, F.A. RODRIGUES, G. TRAVIESO, P.R.V. BOAS, *Characterization of complex networks: A survey of measurements*. Advances in Physics 56, 167–242 (2005)
- S.N. DOROGOVTSSEV, J.F.F. MENDES, *Evolution of Networks*, vol. 1, 1st edn. (Oxford University Press, New York, 2003), p. 264
- S.N. DOROGOVTSSEV, A.V. GOLTSEV, J.F.F. MENDES, *Critical phenomena in complex networks*80, 1275–1335 (2008)

- R. GERMANO, A.P.S. DE MOURA, *Traffic of particles in complex networks*. Phys. Rev. E 74, 036117 (2006)
- H.O. GHAFARI, R.P. YOUNG, *Acoustic-friction networks and the evolution of precursor rupture fronts in laboratory earthquakes*. Sci. Rep. 3(1799), 1–6 (2013)
- M.L. GOLDSTEIN, S.A. MORRIS, G.G. YEN, *Problems with fitting to the power-law distribution*. Eur. Phys. J. B 41, 255–258 (2004)
- A. GRUZD, B. WELLMAN, Y. TAKHTEYEV, *Imagining twitter as an imagined community*. American Behavioral Scientist 55(10), 1294–1318 (2011)
- M. KITSAK, S. HAVLIN, G. PAUL, M. RICCABONI, F. PAMMOLLI, H.E. STANLEY, *Betweenness centrality of fractal and nonfractal scale-free model networks and tests on real networks*. Phys. Rev. E 75(056115), 1–8 (2007)
- L. LACASA, B. LUQUE, J. LUQUE, J.C. NUÑO, *The visibility graph: A new method for estimating the hurst exponent of fractional brownian motion*. A Lett. Jour. Explor. the Front. of Phys. 86(30001), 1–5 (2009)
- M.E.J. NEWMAN, *Assortative mixing in networks*. Phys. Rev. Lett. 89(20), 208701 (2002)
- M.E.J. NEWMAN, *A measure of betweenness centrality based on random walks*. Social Networks 27, 39–54 (2005)
- M.E.J. NEWMAN, M. GIRVAN, *Finding and evaluating community structure in networks*. Phys. Rev. E 69(026113), 1–15 (2004)
- G. PALLA, I. DERÉNYI, I. FARKAS, T. VICSEK, *Uncovering the overlapping community structure of complex networks in nature and society*. Nature 435, 814–818 (2005)
- L. TELESCA, M. LOVALLO, *Analysis of seismic sequences by using the method of visibility graph* 97, 50002–1500024 (2012)

(Received November 30, 2015, accepted June 14, 2016, Published online June 25, 2016)